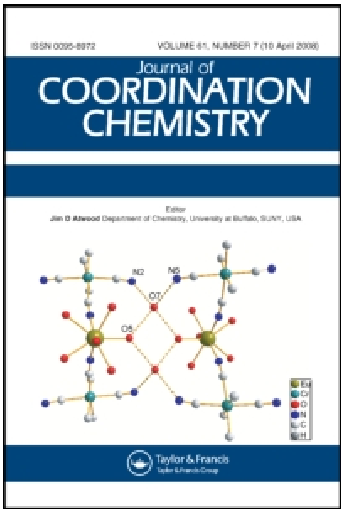

Journal of Coordination Chemistry
Publication details, including instructions for authors and subscription information:
http://www.informaworld.com/smpp/title~content=t713455674

Syntheses, structural determination, and binding studies of nine-coordinate $(enH_2)_3[Tb^{III}(ttha)]_2\cdot 11H_2O$ and eight- coordinate $(enH_2)[Tb^{III}(pdta)(H_2O)]_2\cdot 8H_2O$

Jun Wang[a]; Dan Li[a]; Jingqun Gao[a]; Bin Liu[b]; Baoxin Wang[a]; Dan Wang[b]; Tingting Fan[b]; Xiangdong Zhang[a]
[a] Department of Chemistry, Liaoning University, Shenyang 110036, P.R. China [b] Department of Pharmacy, Liaoning University, Shenyang 110036, P.R. China

First published on: 04 October 2010

To cite this Article Wang, Jun , Li, Dan , Gao, Jingqun , Liu, Bin , Wang, Baoxin , Wang, Dan , Fan, Tingting and Zhang, Xiangdong(2010) 'Syntheses, structural determination, and binding studies of nine-coordinate $(enH_2)_3[Tb^{III}(ttha)]_2\cdot 11H_2O$ and eight- coordinate $(enH_2)[Tb^{III}(pdta)(H_2O)]_2\cdot 8H_2O$', Journal of Coordination Chemistry, 63: 21, 3792 — 3804, First published on: 04 October 2010 (iFirst)

To link to this Article: DOI: 10.1080/00958972.2010.521240
URL: http://dx.doi.org/10.1080/00958972.2010.521240

Journal of Coordination Chemistry
Vol. 63, No. 21, 10 November 2010, 3792–3804

Syntheses, structural determination, and binding studies of nine-coordinate $(enH_2)_3[Tb^{III}(ttha)]_2 \cdot 11H_2O$ and eight-coordinate $(enH_2)[Tb^{III}(pdta)(H_2O)]_2 \cdot 8H_2O$

JUN WANG*†, DAN LI†, JINGQUN GAO†, BIN LIU‡, BAOXIN WANG†, DAN WANG‡, TINGTING FAN‡ and XIANGDONG ZHANG†

†Department of Chemistry, Liaoning University, Shenyang 110036, P.R. China
‡Department of Pharmacy, Liaoning University, Shenyang 110036, P.R. China

(*Received 25 January 2010; in final form 16 July 2010*)

Two complexes, $(enH_2)_3[Tb^{III}(ttha)]_2 \cdot 11H_2O$ (**1**) (en = ethylenediamine and H_6ttha = triethylenetetramine-$N, N, N', N'', N''', N'''$-hexaacetic acid) and $(enH_2)[Tb^{III}(pdta)(H_2O)]_2 \cdot 8H_2O$ (**2**) (H_4pdta = propylenediamine-N, N, N', N'-tetraacetic acid), were synthesized and characterized by elemental analysis, infrared spectrum, UV-Vis spectrum, fluorescence spectrum, and single-crystal X-ray diffraction. The central Tb^{III} of **1** is nine-coordinate, pseudo-monocapped square antiprism with four nitrogens and five oxygens from one ttha, and crystallizing in the monoclinic crystal system with $P2_1/n$ space group. There is a free (non-coordinate) carboxylate ($–CH_2COO^-$) in the $[Tb^{III}(ttha)]^{3-}$. The central Tb^{III} of **2** is eight-coordinate in a standard square antiprism with two nitrogens and four oxygens of one pdta, one oxygen from a carboxylate of an adjacent pdta, and one oxygen from water, crystallizing in the monoclinic crystal system with $C2/c$ space group. Binding between the enH_2^{2+} with $[Tb^{III}(ttha)]^{3-}$ or $[Tb^{III}(pdta)(H_2O)]^-$ is reviewed, providing the basis for interaction of Tb^{III} complexes with biomolecules.

Keywords: Tb^{III} ion; Triethylenetetramine-$N, N, N', N'', N''', N'''$-hexaacetic acid ($H_6$ttha); Propylenediamine-$N, N, N', N'$-tetraacetic acid ($H_4$pdta); Ethylenediamine (en); Hydrogen bond

1. Introduction

Rare earth (RE) metal complexes, due to their widespread applications in pharmacochemistry, biochemistry, material chemistry, and so forth [1, 2], have attracted comprehensive attention among chemists. Especially, Tb^{III} complexes, with distinct luminescence hypersensitivity to the environment, narrow bandwidth, and long-lived emissions [3–9], are of great interest in the applications to fluorescent lighting and as probes in biological systems [10, 11]. Distinct fluorescence and diverse applications originated from the molecular structures of RE metal complexes. Generally, RE^{3+} ions

*Corresponding author. Email: wangjuncomplex890@126.com

Journal of Coordination Chemistry
ISSN 0095-8972 print/ISSN 1029-0389 online
DOI: 10.1080/00958972.2010.521240

with large radii coordinate with N donors or O donors; ligands with both nitrogens and COOH groups are extensively exploited to synthesize stable and soluble RE metal complexes. Therefore, two aminopolycarboxylic ligands, H_6ttha (= triethylenetetramine-$N, N, N', N'', N''', N'''$-hexaacetic acid) and H_4pdta (= propylenediamine-N, N, N', N'-tetraacetic acid), both containing nitrogen and COOH were used to synthesize two RE metal complexes.

The structure and coordination number of RE metal complexes relates to ionic radii, electronic configuration, and oxidation state of the center metal [12, 13]. Complexes of RE metals can adopt eight-, nine-, and ten-coordinate structures with various aminopolycarboxylic acids [14–18]. RE metal ions (such as La^{III}, Ce^{III}, Pr^{III}, Nd^{III}, and Pm^{III}) having large radii usually form high (ten-) coordinate complexes. On the contrary, RE metal ions (such as Ho^{III}, Er^{III}, Tm^{III}, Yb^{III}, and Lu^{III}) having small radii form low (eight-) coordinate complexes. Thus, Tb^{III}, as an in-between RE metal ion (Sm^{III}, Eu^{III}, Gd^{III}, Tb^{III}, and Dy^{III}), possessing ionic radius of 1.063 Å (when the coordination number is six), and high-spin f^8, is more likely to form nine-coordinate complexes. Ligand structures also play a vital effect on the structure and coordination number of RE metal complexes. Ttha, a decadentate ligand, has strong chelating ability to form high-coordinate complexes with large RE metal ions, while the pdta as a hexadentate ligand having a longer propane group should form low-coordinate complexes with RE metal ions. Hence, the Tb^{III} ion has more opportunity to form a nine-coordinate structure with ttha ligand, but an eight-coordinate structure with pdta ligand. That is, a six-membered ring in the complex of the Tb^{III} ion with pdta ligand makes it more difficult to form a nine-coordinate structure.

In order to get deeper insight into the Tb^{III} complexes with ttha and pdta ligands and the effects caused by their differences, **1** and **2** were synthesized to compare their crystal and molecular structures. As expected, $(enH_2)_3[Tb^{III}(ttha)]_2 \cdot 11H_2O$ is nine-coordinate, while $(enH_2)[Tb^{III}(pdta)(H_2O)]_2 \cdot 8H_2O$ is eight-coordinate. This study supports the idea that the structures of the RE metal complexes with aminopolycarboxylic acid are mainly determined by radii of the central metal ions, electron configuration, and ligand structures. Binding between enH_2^{2+} with $[Tb^{III}(ttha)]^{3-}$ and $[Tb^{III}(pdta)(H_2O)]^{-}$ is reviewed, providing the basis for the interaction of Tb^{III} complexes with various biomolecules.

2. Experimental

2.1. *Syntheses*

2.1.1. $(enH_2)_3[Tb^{III}(ttha)]_2 \cdot 11H_2O$ (1). H_6ttha (= triethylenetetramine-$N, N, N', N'', N''', N'''$-hexaacetic acid) (A.R., Beijing SHLHT Science & Trade Co., Ltd., China) (4.9446 g, 10.0 mmol) was added to 100 mL warm water and Tb_4O_7 powder (99.999%, Yuelong Rare Earth Co., Ltd., China) (1.8692 g, 2.5 mmol) was slowly added to the above solution. The solution became transparent after the mixture was stirred and refluxed for 15.0 h, and then the pH was adjusted to 6.0 by dilute ethylenediamine (en) aqueous solution. Finally, the solution was concentrated to 25 mL. Light-yellow crystals appeared after 3 weeks at room temperature. Anal. Found (%): Tb 18.76, C 29.78, H 6.04, N 11.57; Calcd (%): Tb 18.73, C 29.72, H 6.05, N 11.55. The formula ($TbC_{21}H_{51}N_7O_{18}$) is consistent with the result of X-ray diffraction analysis.

2.1.2. $(enH_2)[Tb^{III}(pdta)(H_2O)]_2 \cdot 8H_2O$ (2). H_4pdta (= propylenediamine-*N*, *N*, *N*′, *N*′-tetraacetic acid) (A.R., Beijing SHLHT Science & Trade Co., Ltd., China) (3.0627 g, 10.0 mmol) was added to 100 mL warm water and Tb_4O_7 powder (1.8692 g, 2.5 mmol) was slowly added to the solution. The solution became transparent after the mixture was stirred and refluxed for 18.0 h, and then the pH was adjusted to 6.0 by dilute ethylenediamine (en) aqueous solution. Finally, the solution was concentrated to 25 mL and light-yellow crystals appeared after 2 weeks at room temperature. Anal. Found (%): Tb 27.29, C 24.75, H 5.01, N 7.21; Calcd (%): Tb 27.29, C 24.75, H 5.02, N 7.22. The formula ($TbC_{12}H_{29}N_3O_{13}$) is consistent with the result of X-ray diffraction analysis.

2.2. *FT-IR spectra determination*

H_6ttha, H_4pdta, $(enH_2)_3[Tb^{III}(ttha)]_2 \cdot 11H_2O$ (**1**), and $(enH_2)[Tb^{III}(pdta)(H_2O)]_2 \cdot 8H_2O$ (**2**) samples were skived and pressed to pellets with KBr and their spectra were determined on a Shimadza-IR 408 spectrograph. The obtained results are shown in the "Supplementary material" section.

2.3. *UV-Vis and fluorescence spectra determination*

UV-Vis and fluorescence spectra of $(enH_2)_3[Tb^{III}(ttha)]_2 \cdot 11H_2O$ (**1**) and $(enH_2)[Tb^{III}(pdta)(H_2O)]_2 \cdot 8H_2O$ (**2**) solutions were determined at room temperature by a Cary-50 UV-Vis spectrophotometer and Cary-300 fluorescence spectrophotometer. The results are given in figure 1.

2.4. *X-ray structure determination*

X-ray intensity data were collected on a Bruker SMART CCD type X-ray diffractometer system with graphite-monochromated Mo-Kα radiation ($\lambda = 0.71073$ Å). The structure was solved by direct methods. All non-hydrogen atoms were refined anisotropically by full-matrix least-squares. All calculations were performed by the SHELXTL-97 program on PDP11/44 and Pentium MMX/166 computers. Figures 2 and 3 illustrate perspective views of two complexes. Figures 4 and 5 display their molecular packing in a unit cell. Figures 6 and 7 present the inner hydrogen bonds in **1** and **2**. Figure 8 gives the extended 1-D zigzag chain structure of **2**. Crystal data and structure refinement for **1** and **2** are listed in table 1, and selected bond distances and angles are given in table 2. Final atomic coordinates and equivalent isotropic displacement parameters for all the non-hydrogen fractions are provided in the "Supplementary material (table S1)" for **1** and **2**.

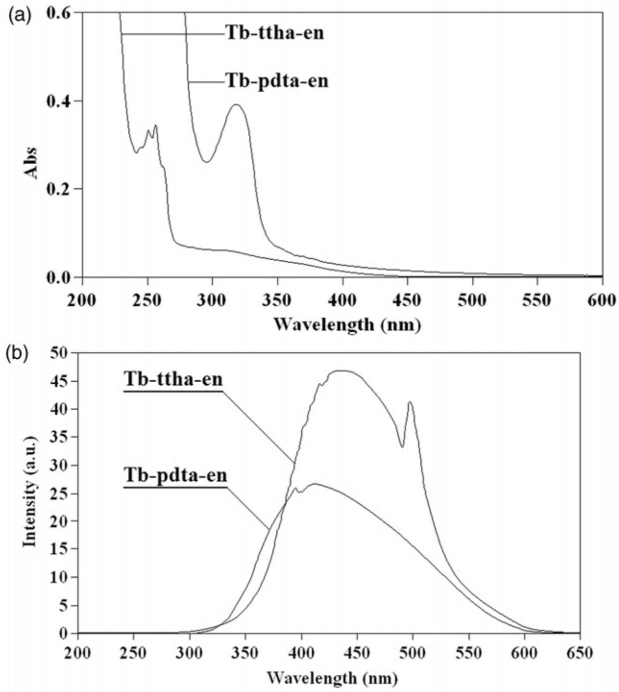

Figure 1. UV-Vis (a) and fluorescence (b) spectra of $(enH_2)_3[Tb^{III}(ttha)]_2 \cdot 11H_2O$ (**1**) and $(enH_2)[Tb^{III}(pdta)(H_2O)]_2 \cdot 8H_2O$ (**2**).

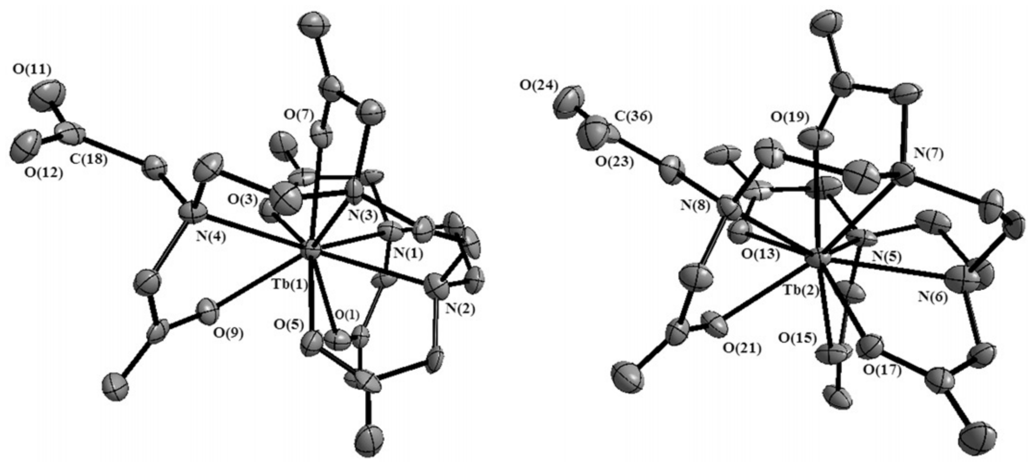

Figure 2. The structure of $[Tb^{III}(ttha)]_2^{6-}$ in **1**.

3. Results and discussion

3.1. *FT-IR spectra*

3.1.1. $(enH_2)_3[Tb^{III}(ttha)]_2 \cdot 11H_2O$ (1). A comparison of FT-IR spectra between H_6ttha and $(enH_2)_3[Tb^{III}(ttha)]_2 \cdot 11H_2O$ (**1**) reveals (Supplementary material) that

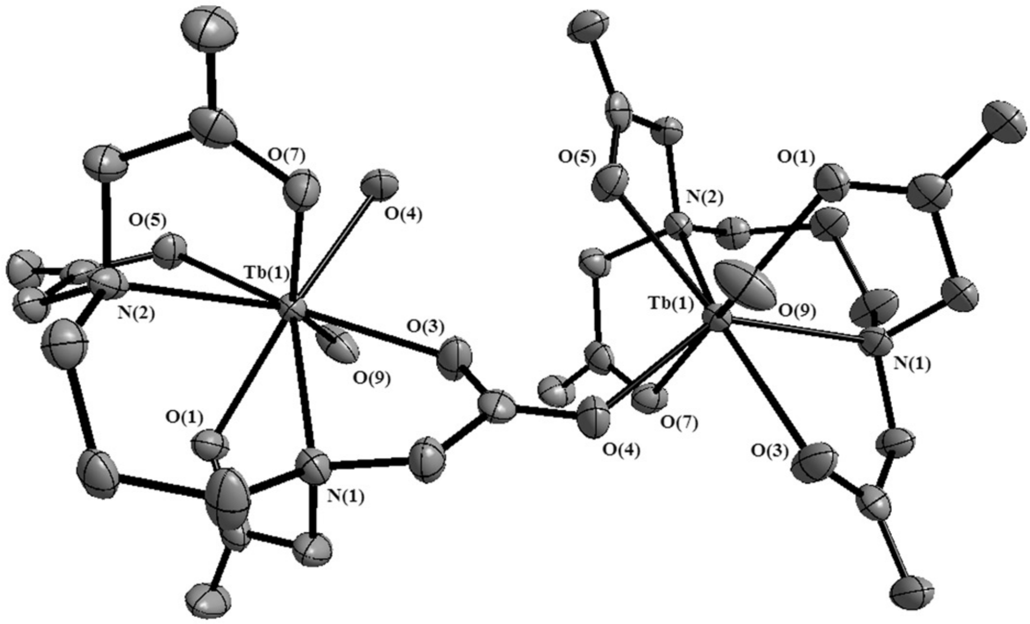

Figure 3. The structure of $[Tb^{III}(pdta)(H_2O)]_2^{2-}$ in **2**.

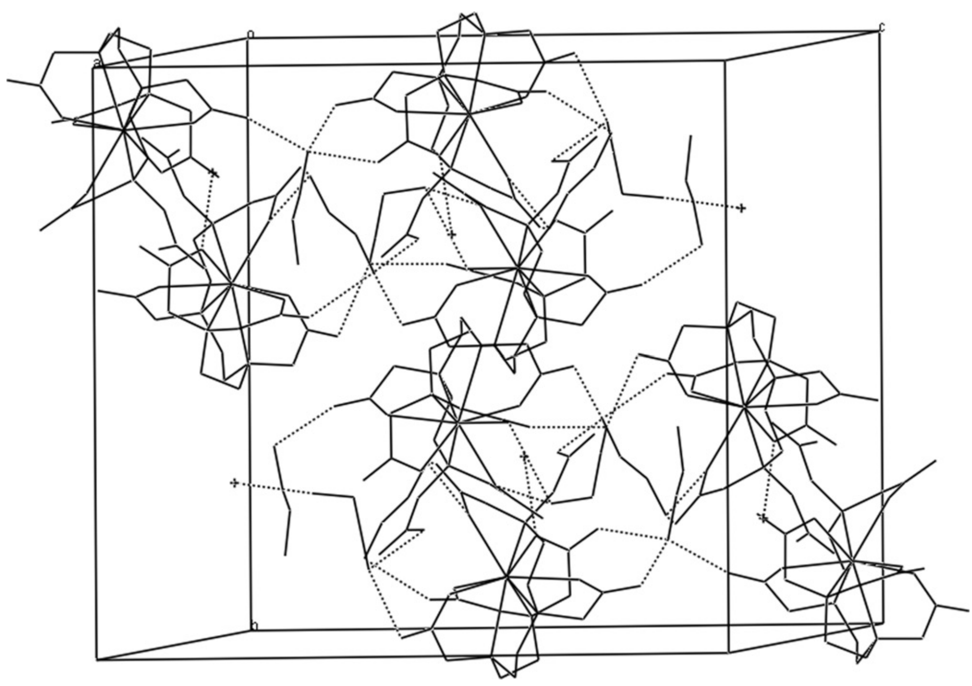

Figure 4. Arrangement of **1** in unit cell (dashed lines represent intermolecular hydrogen bonds).

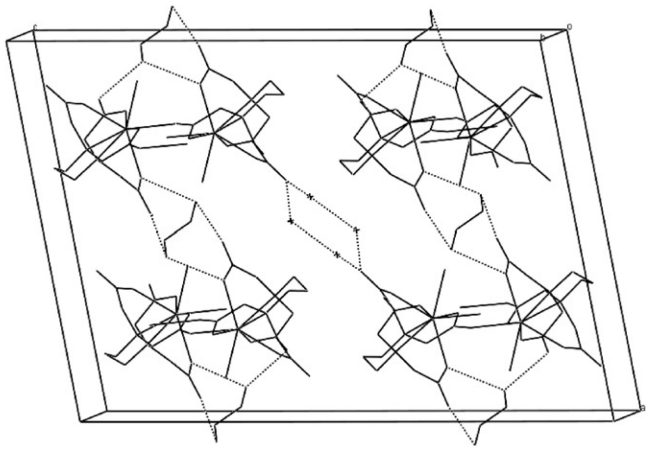

Figure 5. Arrangement of **2** in unit cell (dashed lines represent intermolecular hydrogen bonds).

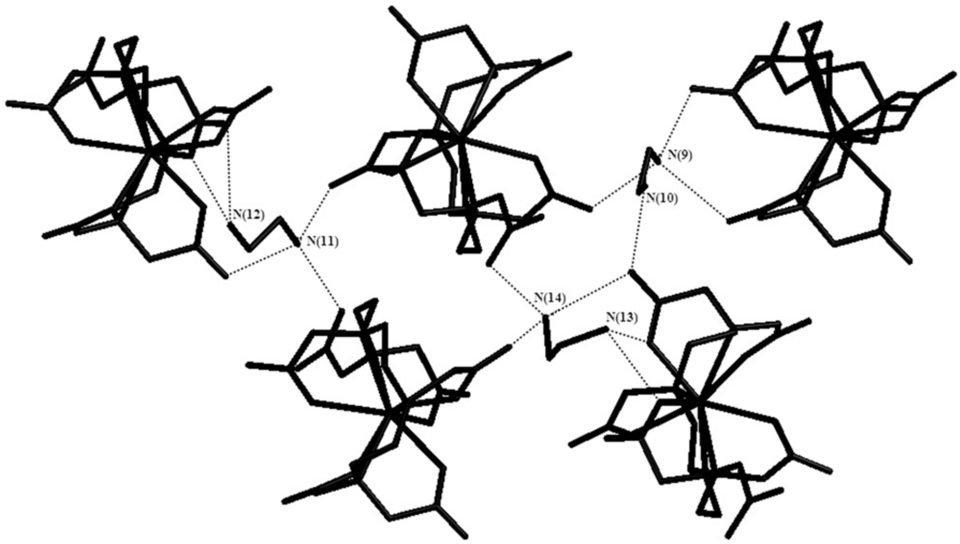

Figure 6. Bindings between enH_2^{2+} and $[Tb^{III}(ttha)]^{3-}$ (dashed lines represent intermolecular hydrogen bonds).

ν(C–N) of $(enH_2)_3[Tb^{III}(ttha)]_2 \cdot 11H_2O$ at 1279 cm^{-1} displays a blue-shift (59 cm^{-1}) compared with that (1220 cm^{-1}) of H_6ttha, indicating that amine nitrogens of ttha are coordinated to Tb^{III}. The ν_{as}(COOH) of H_6ttha at 1738 cm^{-1} disappears in FT-IR spectrum of **1**. ν_{as}(COO) of **1** appears at 1590 cm^{-1}, revealing a blue-shift (33 cm^{-1}) compared with that (1557 cm^{-1}) of H_6ttha. The ν_s(COO) of **1** at 1410 cm^{-1} shows a red-shift (14 cm^{-1}) compared with that (1424 cm^{-1}) of H_6ttha. These changes confirm that oxygens from carboxylate are also coordinated to Tb^{III}. In addition, a broad ν(OH) near 3448 cm^{-1} reveals the presence of H_2O in **1**.

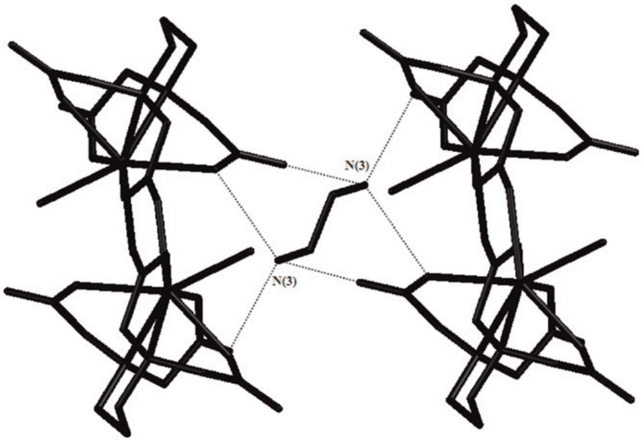

Figure 7. Binding between enH_2^{2+} and $[Tb^{III}(pdta)(H_2O)]^-$ (dashed lines represent intermolecular hydrogen bonds).

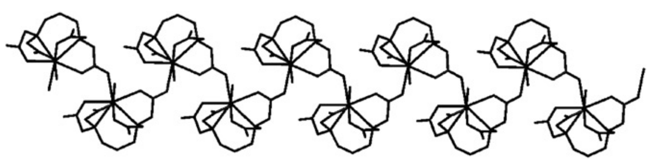

Figure 8. Extended 1-D zigzag chains of **2**.

3.1.2. $(enH_2)[Tb^{III}(pdta)(H_2O)]_2 \cdot 8H_2O$ (2). The ν(C–N) of $(enH_2)[Tb^{III}(pdta)(H_2O)]_2 \cdot 8H_2O$ (**2**) at 1102 cm^{-1} displays a blue-shift (34 cm^{-1}) compared with that (1068 cm^{-1}) of H_4pdta, suggesting that amine nitrogens of pdta are coordinated to Tb^{III}. ν_{as}(COOH) of H_4pdta at 1733 cm^{-1} disappears in the spectrum of **2**. The ν_s(COO) of **2** at 1444 cm^{-1} is blue-shifted (29 cm^{-1}) compared with that (1415 cm^{-1}) of H_4pdta; ν_{as}(COO) of **2** appears at 1595 cm^{-1}, showing a red-shift (67 cm^{-1}) compared with that (1662 cm^{-1}) of H_4pdta. These changes indicate that oxygens from carboxylate are also coordinated to Tb^{III}. A broad ν(OH) near 3432 cm^{-1} reveals the existence of H_2O in **2**.

3.2. *UV-Vis and fluorescence spectra*

UV-Vis spectra of **1** and **2** are depicted in figure 1(a). With the different ligands (ttha and pdta), the maximum absorption peaks appear at 250 and 256 nm for **1** and 320 nm for **2** because the strong nine-coordinate crystal field causes the absorption to move toward the ultraviolet region. The absorptions are probably f–d transitions for both complexes.

As shown in figure 1(b), emission spectra of **1** and **2** in water at room temperature give broad emission bands between 300 and 600 nm, with maximum emissions at 434 and 408 nm, respectively. The maximum emissions may be attributed to $^5D_4$–$^7F_6$ transitions for both $(enH_2)_3[Tb^{III}(ttha)]_2 \cdot 11H_2O$ and $(enH_2)[Tb^{III}(pdta)(H_2O)]_2 \cdot 8H_2O$.

Table 1. Crystal data and structure refinement for **1** and **2**.

Complex	**1**	**2**
Formula weight	839.60	582.30
Temperature (K)	93(2)	93(2)
Wavelength (Å)	0.71073	0.71073
Crystal system	Monoclinic	Monoclinic
Space group	$P2_1/n$	$C2/c$
Unit cell dimensions (Å, °)		
a	17.7357(19)	18.144(2)
b	19.239(2)	9.2463(10)
c	20.570(2)	25.150(3)
β	111.5890(10)	100.588(2)
Volume (Å^3), Z	6526.5(12), 8	4147.3(8), 8
Calculated density (mg m^{-3})	1.709	1.865
Absorption coefficient (mm^{-1})	2.253	3.479
F(000)	3440	2328
Crystal size (mm^3)	$0.43 \times 0.33 \times 0.30$	$0.30 \times 0.27 \times 0.27$
θ_{range} for data collection (°)	3.00–25.00	3.05–27.50
Limiting indices	$-18 \le h \le 21$; $-22 \le k \le 19$; $-24 \le l \le 24$	$-18 \le h \le 23$; $-11 \le k \le 11$; $-32 \le l \le 32$
Reflections collected	41,163	16,322
Independent reflections	11,427 [R(int) = 0.0520]	4754 [R(int) = 0.0227]
Completeness to $\theta_{\max}$ (%)	99.4	99.6
Max. and min. transmission	0.5514 and 0.4421	0.4568 and 0.4217
Goodness-of-fit on F^2	1.190	1.002
Final R indices [$I > 2\sigma(I)$]	$R_1 = 0.0447$, $wR_2 = 0.0925$	$R_1 = 0.0196$, $wR_2 = 0.0431$
R indices (all data)	$R_1 = 0.0479$, $wR_2 = 0.0940$	$R_1 = 0.0223$, $wR_2 = 0.0445$
Largest difference peak and hole (e Å^{-3})	1.967 and −1.017	1.746 and −0.419
Absorption correction	Empirical	Empirical
Refinement method	Full-matrix least-squares on F^2	Full-matrix least-squares on F^2

3.3. *Molecular and crystal structures*

3.3.1. $(enH_2)_3[Tb^{III}(ttha)]_2 \cdot 11H_2O$ (1). One bridging water (O(29)) links two different $[Tb^{III}(ttha)]^{3-}$ complex anions through hydrogen bonds. Each Tb^{III} is nine-coordinate (figure 2) with four nitrogens and five oxygens, all from one ttha. As in $[Dy^{III}(ttha)]^{3-}$ [19], $[Ho^{III}(ttha)]^{3-}$ [19], and $[Er^{III}(ttha)]^{3-}$ [19], each TbN_2O_7 in $[Tb^{III}(ttha)]_2^{6-}$ has a free carboxylate, O(11)–C(12)–O(18), and O(23)–C(36)–O(24), which could be modified by functional groups or biological molecules. The geometry around Tb^{III}(1) can be considered as nine-coordinate pseudo-monocapped square antiprismatic. The coordinate atoms around Tb^{III}(1) form two approximate parallel planes: the set of O(1), O(3), O(5), and N(4), and the set of O(7), N(1), N(2), and N(3) with average torsion angle of the two square planes about 47.93°. The capping position is occupied by O(9) above the plane of O(1), O(3), O(5), and N(4). Repulsion between the capped O(9) and the top plane makes the distance between the two planes shorter than that of a standard square antiprism, as seen from table 2 (bond **1**-a). The Tb^{III}(1)–O bond distances range from 2.339(4) Å (Tb^{III}(1)–O(1) and Tb^{III}(1)–O(7)) to 2.434(4) Å (Tb^{III}(1)–O(3)), with average value of 2.376(4) Å; Tb^{III}(1)–N bond distances range from 2.621(5) Å (Tb^{III}(1)–N(1)) to 2.692(5) Å (Tb^{III}(1)–N(3)), and the average

Table 2. Selected bond distances (Å) and angles (°) of **1** and **2**.

Bond	*d* (Å)	Bond	*d* (Å)	Bond	*d* (Å)
1-a					
Tb(1)–O(1)	2.343(3)	Tb(1)–O(7)	2.340(3)	Tb(1)–N(2)	2.649(4)
Tb(1)–O(3)	2.431(4)	Tb(1)–O(9)	2.374(3)	Tb(1)–N(3)	2.693(4)
Tb(1)–O(5)	2.351(3)	Tb(1)–N(1)	2.617(4)	Tb(1)–N(4)	2.623(4)
1-b					
Tb(2)–O(13)	2.406(4)	Tb(2)–O(19)	2.367(4)	Tb(2)–N(6)	2.646(5)
Tb(2)–O(15)	2.339(3)	Tb(2)–O(21)	2.387(4)	Tb(2)–N(7)	2.719(4)
Tb(2)–O(17)	2.379(3)	Tb(2)–N(5)	2.655(4)	Tb(2)–N(8)	2.675(4)
2					
Tb(1)–O(1)	2.3304(15)	Tb(1)–O(5)	2.3460(15)	Tb(1)–N(1)	2.6531(18)
Tb(1)–O(3)	2.3363(15)	Tb(1)–O(7)	2.3861(16)	Tb(1)–N(2)	2.5930(18)
Tb(1)–O(4)#1	2.3513(16)	Tb(1)–O(9)	2.3676(16)		
Angle	*ω* (°)	Angle	*ω* (°)	Angle	*ω* (°)
1-a					
O(1)–Tb(1)–O(3)	86.46(12)	O(3)–Tb(1)–N(2)	131.63(12)	O(7)–Tb(1)–N(3)	64.97(12)
O(1)–Tb(1)–O(5)	75.19(12)	O(3)–Tb(1)–N(3)	135.88(12)	O(7)–Tb(1)–N(4)	78.19(12)
O(1)–Tb(1)–O(7)	143.97(12)	O(3)–Tb(1)–N(4)	95.49(12)	O(9)–Tb(1)–N(1)	121.00(13)
O(1)–Tb(1)–O(9)	71.87(12)	O(5)–Tb(1)–O(7)	135.96(12)	O(9)–Tb(1)–N(2)	132.11(13)
O(1)–Tb(1)–N(1)	66.03(13)	O(5)–Tb(1)–O(9)	75.19(12)	O(9)–Tb(1)–N(3)	125.59(12)
O(1)–Tb(1)–N(2)	71.52(13)	O(5)–Tb(1)–N(1)	127.27(13)	O(9)–Tb(1)–N(4)	64.14(12)
O(1)–Tb(1)–N(3)	134.83(12)	O(5)–Tb(1)–N(2)	66.41(12)	N(1)–Tb(1)–N(2)	68.25(13)
O(1)–Tb(1)–N(4)	133.58(12)	O(5)–Tb(1)–N(3)	71.56(12)	N(1)–Tb(1)–N(3)	113.40(13)
O(3)–Tb(1)–O(5)	148.46(12)	O(5)–Tb(1)–N(4)	79.92(12)	N(1)–Tb(1)–N(4)	152.61(13)
O(3)–Tb(1)–O(7)	71.69(12)	O(7)–Tb(1)–O(9)	125.93(12)	N(2)–Tb(1)–N(3)	67.61(13)
O(3)–Tb(1)–O(9)	74.80(12)	O(7)–Tb(1)–N(1)	78.49(13)	N(2)–Tb(1)–N(4)	130.98(13)
O(3)–Tb(1)–N(1)	63.46(13)	O(7)–Tb(1)–N(2)	101.75(13)	N(3)–Tb(1)–N(4)	68.52(13)
1-b					
O(13)–Tb(2)–O(15)	83.51(12)	O(15)–Tb(2)–N(6)	74.20(13)	O(19)–Tb(2)–N(7)	63.65(12)
O(13)–Tb(2)–O(17)	149.95(12)	O(15)–Tb(2)–N(7)	138.67(13)	O(19)–Tb(2)–N(8)	75.56(13)
O(13)–Tb(2)–O(19)	71.22(12)	O(15)–Tb(2)–N(8)	138.05(12)	O(21)–Tb(2)–N(5)	124.27(13)
O(13)–Tb(2)–O(21)	74.10(13)	O(17)–Tb(2)–O(19)	136.38(12)	O(21)–Tb(2)–N(6)	137.69(13)
O(13)–Tb(2)–N(5)	62.84(14)	O(17)–Tb(2)–O(21)	78.60(12)	O(21)–Tb(2)–N(7)	124.63(12)
O(13)–Tb(2)–N(6)	129.87(13)	O(17)–Tb(2)–N(5)	127.22(13)	O(21)–Tb(2)–N(8)	63.80(12)
O(13)–Tb(2)–N(7)	134.02(12)	O(17)–Tb(2)–N(6)	66.65(12)	N(5)–Tb(2)–N(6)	67.11(14)
O(13)–Tb(2)–N(8)	94.14(13)	O(17)–Tb(2)–N(7)	72.89(12)	N(5)–Tb(2)–N(7)	110.77(13)
O(15)–Tb(2)–O(17)	77.66(12)	O(17)–Tb(2)–N(8)	84.76(12)	N(5)–Tb(2)–N(8)	146.99(13)
O(15)–Tb(2)–O(19)	140.24(12)	O(19)–Tb(2)–O(21)	123.34(13)	N(6)–Tb(2)–N(7)	67.83(13)
O(15)–Tb(2)–O(21)	75.45(12)	O(19)–Tb(2)–N(5)	74.67(13)	N(6)–Tb(2)–N(8)	131.93(13)
O(15)–Tb(2)–N(5)	66.49(12)	O(19)–Tb(2)–N(6)	98.76(13)	N(7)–Tb(2)–N(8)	67.14(13)
2					
O(1)–Tb(1)–O(3)	104.65(5)	O(3)–Tb(1)–O(9)	78.13(6)	O(5)–Tb(1)–N(1)	135.00(5)
O(1)–Tb(1)–O(4)#1	143.22(5)	O(3)–Tb(1)–N(1)	65.44(5)	O(5)–Tb(1)–N(2)	65.24(5)
O(1)–Tb(1)–O(5)	77.27(5)	O(3)–Tb(1)–N(2)	140.88(6)	O(7)–Tb(1)–O(9)	84.52(5)
O(1)–Tb(1)–O(7)	136.98(5)	O(4)#1–Tb(1)–O(5)	78.97(5)	O(7)–Tb(1)–N(1)	65.45(5)
O(1)–Tb(1)–O(9)	72.85(6)	O(4)#1–Tb(1)–O(7)	71.67(6)	O(7)–Tb(1)–N(2)	150.17(6)
O(1)–Tb(1)–N(1)	66.90(5)	O(4)#1–Tb(1)–O(9)	138.81(5)	O(9)–Tb(1)–N(1)	114.41(6)
O(1)–Tb(1)–N(2)	78.44(5)	O(4)#1–Tb(1)–N(1)	123.58(6)	O(9)–Tb(1)–N(2)	137.10(6)
O(3)–Tb(1)–O(4)#1	77.17(5)	O(4)#1–Tb(1)–N(2)	86.01(5)	N(1)–Tb(1)–N(2)	81.20(6)
O(3)–Tb(1)–O(5)	153.88(5)	O(5)–Tb(1)–O(7)	105.86(5)		
O(3)–Tb(1)–O(7)	90.54(5)	O(5)–Tb(1)–O(9)	77.66(6)		

value is 2.645(4) Å, remarkably longer than the mean value of $Tb^{III}(1)$–O distance, suggesting that $Tb^{III}(1)$–O bonds are much more stable than $Tb^{III}(1)$–N bonds.

Average value of the angles (∠O(1)Tb^{III}(1)O(9), ∠O(3)Tb^{III}(1)O(9), ∠O(5)Tb^{III}(1)O(9), and ∠N(4)Tb^{III}(1)O(9)) is 71.50°, in which the biggest and smallest are 75.31° and 64.09°, close to 70° as for most complexes with nine-coordinate pseudo-monocapped square antiprismatic structures. The dihedral angles for the top plane are 14.93° between triangle Δ(O(1)O(3)N(4)) and triangle Δ(O(1)O(5)N(4)), and 14.97° between triangle Δ(O(1)O(3)O(5)) and triangle Δ(O(3)O(5)N(4)). To the bottom plane, the dihedral angles are 5.65° between triangle Δ(N(1)N(2)O(7)) and triangle Δ(N(2)N(3)O(7)) and 6.45° between triangle Δ(O(7)N(1)N(3)) and triangle Δ(N(1) N(2)N(3)), respectively. According to these data, and on the basis of the definition of nine-coordinate complex given by Guggenberger and Muetterties [20], we firmly conclude that, like most of nine-coordinate RE metal complexes with ttha [21, 22], the conformation around $Tb^{III}(1)$ is a pseudo-monocapped square antiprism.

The coordination environment around $Tb^{III}(2)$ is similar to that of $Tb^{III}(1)$, however, there are some marked differences between them in bond distances and bond angles. The set of O(13), O(15), O(17), and N(8) and the set of N(5), N(6), N(7), and O(19) form two approximate square planes, yielding a square antiprism. The average torsion angle of the two square planes is about 48.15°. The capping position is occupied by O(21) above the plane of O(13), O(15), O(17), and N(8), which repulses these four atoms causing the two planes to close slightly. As seen from table 2 (bond **1**-b), the $Tb^{III}(2)$–O bond distances range from 2.340(4) Å ($Tb^{III}(2)$–O(15)) to 2.404(4) Å ($Tb^{III}(2)$–O(13)), with the average value of 2.375(4) Å; the four $Tb^{III}(2)$–N bond distances vary from 2.645(5) Å ($Tb^{III}(2)$–N(6)) to 2.719(4) Å ($Tb^{III}(2)$–N(7)), with the average value of 2.674(5) Å, much longer than the average $Tb^{III}(2)$–O bonds. The bond distances Tb^{III}–O and Tb^{III}–N around $Tb^{III}(1)$ and $Tb^{III}(2)$ in $(enH_2)_3[Tb^{III}(ttha)]_2 \cdot 11H_2O$ are considerably different, apparently from the influence of crystal water molecules.

In addition, the average values of the angles (∠O(13)Tb(2)O(21), ∠O(15)Tb(2)O(21), ∠O(17)Tb(2)O(21), and ∠N(8)Tb(2)O(21)) is 72.95° close to 70°. The results given in this article and the ones reported previously indicate that the Tb^{III} forms nine-coordinate complexes with aminopolycarboxylic acids due to ionic radius of 1.063 Å and chelating rings are five-membered in the complex structure. To the top plane, the dihedral angles are 14.12° between triangle Δ(O(13)O(15)N(8)) and triangle Δ(O(15)O(17)N(8)), and 14.17° between triangle Δ(O(13)O(15)O(17)) and triangle Δ(O(13)N(8)O(17)). To the bottom plane, the dihedral angles are 5.89° between triangle Δ(N(5)N(6)N(7)) and triangle Δ(N(5)O(19)N(7)), and 5.08° between triangle Δ(N(5)N(6)O(19)) and triangle Δ(N(6)N(7)O(19)). Therefore, the conformation around $Tb^{III}(2)$, like around $Tb^{III}(1)$, is pseudo-monocapped square antiprism.

In previous study, we documented syntheses and structures of $K_4[Tb_2^{III}(Httha)_2] \cdot 14H_2O$ [19] and $(NH_4)_3[Tb^{III}(ttha)] \cdot 5H_2O$ [23] which adopt nine-coordinate binuclear and mononuclear structures, respectively. In the present work, ethylenediamine (en) as the counter ion interacts with $[Tb^{III}(ttha)]^{3-}$, yielding $(enH_2)_3[Tb^{III}(ttha)]_2 \cdot 11H_2O$, mononuclear nine-coordinate. Therefore, if biomolecules, like amino acids, interact with $[Tb^{III}(ttha)]^{3-}$, a series of nine-coordinate mononuclear complexes could also be formed.

As shown in figure 4, there are eight $(enH_2)_3[Tb^{III}(ttha)]_2 \cdot 11H_2O$ molecules in a unit cell. The molecules connect with each other through hydrogen bonds and electrostatic bonding with crystal water and ethylenediamine cations (enH_2^{2+}), forming a net structure. The crystal waters associate with $[Tb^{III}(ttha)]^{3-}$ through hydrogen bonds *via* carboxylate of ttha and connect with enH_2^{2+} cations through hydrogen bonds and electrostatic forces. Crystal waters also affect the coordinate structure, leading to a non-standard nine-coordinate pseudo-monocapped square antiprism. All enH_2^{2+} can be separated into three types. The first enH_2^{2+} forms hydrogen bonds with three $[Tb^{III}(ttha)]^{3-}$; N(9) links three oxygens, two from two carboxylates of the same $[Tb^{III}(ttha)]^{3-}$ and one from the other $[Tb^{III}(ttha)]^{3-}$, while N(10) connects only one oxygen from a neighboring $[Tb^{III}(ttha)]^{3-}$. The second enH_2^{2+} forms hydrogen bonds with three $[Tb^{III}(ttha)]^{3-}$ anions; N(11) links three oxygens from three different $[Tb^{III}(ttha)]^{3-}$, but N(12) coordinates oxygens from the same $[Tb^{III}(ttha)]^{3-}$. The third enH_2^{2+} forms hydrogen bonds with three $[Tb^{III}(ttha)]^{3-}$ anions. Like N(12), N(13) links two oxygens from the same $[Tb^{III}(ttha)]^{3-}$ and N(14) connects three oxygens from three different $[Tb^{III}(ttha)]^{3-}$ anions. Because of different environments, the dihedral angles of these three enH_2^{2+} cations are 161.23°, 71.40°, and 178.13°. First and third enH_2^{2+} cations are close to *trans* configuration, while the second is an unstable Newman structure. Amino acids as part of a protein could interact with $[Tb^{III}(ttha)]^{3-}$ through different binding.

3.3.2. $(enH_2)[Tb^{III}(pdta)(H_2O)]_2 \cdot 8H_2O$ (2). As illustrated in figure 3, a bridging carboxylate (O(3)–C(4)–O(4)) connects two $[Tb^{III}(pdta)(H_2O)]^-$ anions generating a binuclear molecule unit. As shown in figure 8, a catenulate polymer is produced along the *a* axis with $Tb^{III} \cdots Tb^{III}$ distance of 5.821 Å. In each binuclear molecule, Tb^{III} is eight-coordinate by two nitrogens and four oxygens of one pdta, O(4)#1 from a carboxylate of an adjacent pdta, and O(9) from water.

In $[Tb^{III}(pdta)(H_2O)]_2^{2-}$, the $Tb^{III}(1)N_2O_6$ is eight-coordinate with almost standard square antiprism, with O(1), O(3), O(9) (from water molecule) and N(1) and O(4) (from the adjacent pdta ligand), O(5), O(7), and N(2) form two approximately parallel square planes. The average torsion angle between two planes is 45°. Previous RE metal complexes with similar structures, such as $(NH_4)[Eu(pdta)(H_2O)] \cdot H_2O$ [24] and $\{[Sm(Hpdta)(H_2O)] \cdot 2H_2O\}_n$ [25], adopt eight-coordinate square antiprismatic conformations. Tb^{III}(1)–O bond distances (table 2) range from 2.3304(15) Å (Tb^{III}(1)–O(1)) to 2.3861(16) Å (Tb^{III}(1)–O(7)), with an average of 2.3530(16) Å; the two Tb^{III}–N bond distances are 2.6531(18) Å (Tb^{III}(1)–N(1)) and 2.5930(18) Å (Tb^{III}(1)–N(2)), with an average of 2.6231(18) Å. Tb^{III}(1)–O bond distances are significantly shorter than Tb^{III}(1)–N bond distances, suggesting that Tb^{III}(1)–O bonds are much stronger than Tb^{III}(1)–N bonds.

The value of the dihedral angle for the top plane between triangle Δ(O(1)O(3)N(1)) and triangle Δ(O(1)O(3)O(9)) is 2.55° and between triangle Δ(N(1)O(1)O(9)) and triangle Δ(N(1)O(3)O(9)) is 2.91°. To the bottom plane, the value of the dihedral angle between triangle Δ(N(2)O(5)O(7)) and triangle Δ(O(4)O(5)O(7)) is 10.77° and between triangle Δ(O(4)N(2)O(7)) and triangle Δ(N(2)O(4)O(5)) is 12.23°. Judging from these data and according to Guggenberger and Muetterties' method, the conformation around Tb^{III}(1) is a slightly distorted square antiprism.

In one unit cell (figure 5), there are eight $(enH_2)[Tb^{III}(pdta)(H_2O)]_2 \cdot 8H_2O$ molecules, connected through hydrogen bonds and electrostatic bonding with water and protonated enH_2^{2+}. The crystal waters associate with $[Tb^{III}(pdta)(H_2O)]_2^{2-}$ through hydrogen bonds *via* carboxylate of pdta and connect with enH_2^{2+} cations through hydrogen bonds and electrostatic forces (figure 7). One enH_2^{2+} connects four $[Tb^{III}(pdta)(H_2O)]^-$ anions (or two binuclear $[Tb^{III}(pdta)(H_2O)]_2^{2-}$ anions) through hydrogen bonds of N(3) with two uncoordinated and one coordinate oxygens from three different $[Tb^{III}(pdta)(H_2O)]^-$ anions. Hence, all anions link one another through hydrogen bonds of crystal water and enH_2^{2+} cations, yielding a layer structure. Therefore, $[Tb^{III}(pdta)(H_2O)]^-$ and various amino acids could combine through hydrogen bonds and electrostatic interactions, laying the foundation to study the interactions of $[Tb^{III}(pdta)(H_2O)]^-$ with various proteins, small peptides, and amino acids.

4. Conclusions

Two Tb complexes with aminopolycarboxylic acid (H_6ttha = triethylenetetramine-N,N,N',N'',N''',N'''-hexaacetic acid and H_4pdta = propylenediamine-N,N,N',N'-tetraacetic acid) ligands, $(enH_2)_3[Tb^{III}(ttha)]_2 \cdot 11H_2O$ (**1**) and $(enH_2)[Tb^{III}(pdta)(H_2O)]_2 \cdot 8H_2O$ (**2**), have been synthesized. Compound **1** adopts a pseudo-monocapped square antiprismatic nine-coordinate geometry, while **2** adopts a square antiprismatic eight-coordinate polyhedron. Ligand structure and composition play crucial roles in coordination number and complex structure.

Supplementary material

CCDC 748130 $(enH_2)_3[Tb^{III}(ttha)]_2 \cdot 11H_2O$ and CCDC 748129 $(enH_2)[Tb^{III}(pdta)(H_2O)]_2 \cdot 8H_2O$, contain the supplementary crystallographic data for this article. These data can be obtained free of charge *via* www.ccdc.cam.ac.uk/data_request/cif, by e-mailing to data_request@ccdc.cam.ac.uk, or by contacting The Cambridge Crystallographic Data Centre, 12 Union Road, Cambridge CB2 1EZ, UK; Fax: +44(0)1223-336033.

Acknowledgments

The authors greatly acknowledge the National Natural Science Foundation of China, Liaoning Province Natural Science Foundation of Education Department, and Liaoning Province Natural Science Foundation of Science and Technology Department for financial support. The authors also thank our colleagues and other students for their participation in this work. Especially, we thank Professor K. Miyoshi and T. Mizuta (Faculty of Science, Hiroshima University, Japan) for instructions.

References

[1] N. Sabbatini, M. Guardigli, J.M. Lehn. *Coord. Chem. Rev.*, **123**, 201 (1993).
[2] J.C.G. Bunzli, C. Piguet. *Chem. Soc. Rev.*, **34**, 1048 (2005).
[3] F.S. Richardson. *Chem. Rev.*, **82**, 541 (1982).
[4] J.C.G. Bunzli, G.R. Choppin. *Spectrochim Acta, A: Mol. Spectrosc.*, **46**, 1797 (1990).

[5] R.C. Holz, L.C. Thompson. *Inorg. Chem.*, **27**, 4640 (1988).
[6] D. Parker, J.A.G. Williams. *J. Chem. Soc.*, **18**, 3613 (1996).
[7] G.L. Law, K.L. Wong, X. Zhou, W.T. Wong, P.A. Tanner. *Inorg. Chem.*, **44**, 4142 (2005).
[8] S. Petoud, S.M. Cohen, J.C.G. Bunzli, K.N. Raymond. *J. Am. Chem. Soc.*, **125**, 13324 (2003).
[9] G.H. Cui, J.R. Li, R.H. Zhang, X.H. Bu. *J. Mol. Struct.*, **740**, 187 (2005).
[10] X.P. Yang, B.S. Kang, W.K. Wong, C.Y. Sun, H.Q. Liu. *Inorg. Chem.*, **42**, 169 (2003).
[11] M.K. Thompson, M. Vuchkov, I.A. Kahwa. *Inorg. Chem.*, **40**, 4332 (2001).
[12] X. Yu, Q.D. Su. *J. Photochem. Photobio. A: Chem.*, **155**, 73 (2003).
[13] Z. Wang, C.M. Jin, T. Shao. *Inorg. Chem. Commun.*, **5**, 642 (2002).
[14] K. Miyoshi, J. Wang, T. Mizuta. *Bull. Chem. Soc. Jpn.*, **66**, 2547 (1993).
[15] K. Miyoshi, J. Wang, T. Mizuta. *Inorg. Chim. Acta*, **228**, 165 (1995).
[16] J. Wang, X.D. Zhang, Z.R. Liu, W.G. Jia. *J. Mol. Struct.*, **613**, 189 (2002).
[17] J. Wang, X.D. Zhang, Y. Wang, Zh.H. Zhang, Y. Zhang, X.Zh. Liu, L. Wang, H. Li. *Chin. J. Struct. Chem.*, **23**, 1169 (2004).
[18] J. Wang, Y. Wang, Zh.H. Zhang, X.D. Zhang, X.Zh. Liu, L. Wang, H. Li, Zh.J. Pan. *Chin. J. Struct. Chem.*, **23**, 1420 (2004).
[19] J. Wang, Y. Wang, Zh.H. Zhang, X.D. Zhang, X.Y. Liu, X.Zh. Liu, Zh.R. Liu, Y. Zhang, J. Tong, P. Zhang. *J. Coord. Chem.*, **59**, 295 (2006).
[20] L.J. Guggenberger, E.L. Muetterties. *J. Am. Chem. Soc.*, **98**, 7221 (1976).
[21] J. Wang, X.Zh. Liu, Zh.H. Zhang, X.D. Zhang, G.R. Gao, Y.M. Kong, Y. Li. *J. Coord. Chem.*, **59**, 2103 (2006).
[22] J. Wang, X.D. Zhang, W.G. Jia, Y. Zhang, Z.R. Liu. *Russ. J. Coord. Chem.*, **30**, 130 (2004).
[23] J. Wang, X.Zh. Liu, X.F. Wang, G.R. Gao, Zh.Q. Xing, X.D. Zhang, R. Xu. *J. Struct. Chem.*, **49**, 75 (2008).
[24] J. Wang, G.R. Gao, Zh.H. Zhang, X.D. Zhang, X.Zh. Liu, Y.M. Kong, Y. Li. *J. Coord. Chem.*, **59**, 2113 (2006).
[25] J. Wang, P. Hu, B. Liu, X. Chen, L.Q. Zhang, G.X. Han, R. Xu, X.D. Zhang. *Russ. J. Inorg. Chem.*, **55**, 1 (2010).